Revisions to the Discrete Fracture Network Model at Utah FORGE Site

Aleta Finnila[1], Thomas Doe[1], Robert Podgorney[2], Branko Damjanac[3], Pengju Xing[4]

[1] Golder Associates, Redmond, WA, USA

[2] Idaho National Laboratory, Idaho Falls, ID, USA

[3] Itasca Consulting Group, Inc., Minneapolis, MN, USA

[4] Energy & Geoscience Institute, University of Utah, Salt Lake City, UT, USA

Keywords

DFN, FORGE, Milford, Utah, discrete, fracture

ABSTRACT

The Discrete Fracture Network (DFN) model for the Frontier Observatory for Research in Geothermal Energy (FORGE) site near Milford, Utah, is used to characterize the natural fractures present in the reservoir. Subsets of the model are used as initial conditions for researchers simulating processes such as well hydraulic stimulation, local stress evolution, flow pathway analysis, and thermal breakthrough in proposed injection and production well configurations. Image logs from the vertical pilot well, 58-32, along with outcrop data from the nearby Mineral Mountains provided the data used to construct the original DFN model in 2019. Two new wells have been drilled in the past year: a highly deviated injection well, 16A(78)-32, and another deep vertical well, 56-32. Data collected from these wells have been analyzed to further constrain fracture orientations and intensity. Estimates for fracture sizes have been adjusted based on forward modeling work performed on fracture penetration statistics collected from image log data. Mechanical and hydraulic fracture apertures have been estimated for both pre- and post-stimulation states based on pressure history matching of injection well tests and measured values from electrical resistivity logs.

The updated DFN model is presented, and three realizations of the model are uploaded to the U.S. Department of Energy Geothermal Data Repository (GDR) for public access. Each realization includes planar fractures representing both the known location and orientation of fractures identified from the well logs as well as stochastic fracture sets that do not intersect the wells. Individual fracture properties include center coordinates, orientation, fracture size represented both as a radius and as a six-sided polygon, mechanical aperture, hydraulic aperture,

permeability, and compressibility. Fracture properties are calibrated so that the upscaled DFN is consistent with measured bulk rock porosity and permeability.

1. Introduction

FORGE is a multi-year initiative funded by the US Department of Energy (DOE) for testing targeted EGS research and development. The site is located inside the southeast margin of the Great Basin near the town of Milford, Utah, and is described in detail in the Phase 2B Report (EGI, 2018). Current modeling work includes the development of baseline models using Earth, continuum and discrete modeling methods. One of the discrete models being developed is a reference DFN. The initial DFN developed for FORGE was described in 2019 and was based on the data available at the time, primarily data from the vertical pilot well, 58-32, and outcrop data in the nearby mountain range (Finnila et al., 2019). This paper documents the current 2021 DFN model which has been updated based on additional data from two newer wells in the reservoir, a highly deviated injection well, 16A(78)-32, and another deep vertical well, 56-32.

The updated DFN and various subsets of the DFN have been made available to researchers and the public in the GDR. These fracture sets are applicable in, but not limited to well hydraulic stimulation, local stress evolution, flow pathway analysis, and thermal breakthrough in proposed injection and production well configurations. The DFN is also upscaled to provide continuum modelers 3D properties such as fracture porosity, directional permeability and sigma factor.

2. DFN Model Construction

The FORGE reference DFN model was constructed using FracMan software (Golder Associates, 2021). A DFN model explicitly represents fractures in a rock as discrete features. Fractures are represented as planar objects oriented in 3D space with prescribed sizes, shapes, apertures, permeabilities, and compressibilities. The collection of fractures is further described by the number of fractures present and their intensity distribution. Where we know fracture location and orientation, such as at wellbore intersections identified from image log data, the fractures are created in what is termed a deterministic set. Away from measured locations, such as the bulk of the deep FORGE reservoir, fractures are created in stochastic sets where properties are assigned from statistical distributions.

The DFN description is subdivided into four sections: boundaries of the various modeling regions, the stochastic fracture set, the deterministic fracture set, and fracture property calibration.

2.1 Model Regions

There are three model regions used to generate the current DFN models available on the GDR: the largest region is a 4 km x 4 km x 4 km region spanning the full FORGE site from the surface to below the target reservoir region in the granitic bedrock, two smaller regions have been created in order to model well tests performed on Zone 2 of Well 58-32 and stimulation at the toe of well 16A(78)-32. The well-scale model for 58-32 is a cubic region having 300 m sides while the model for 16A(78)-32 is a cubic region having 1000 m sides.

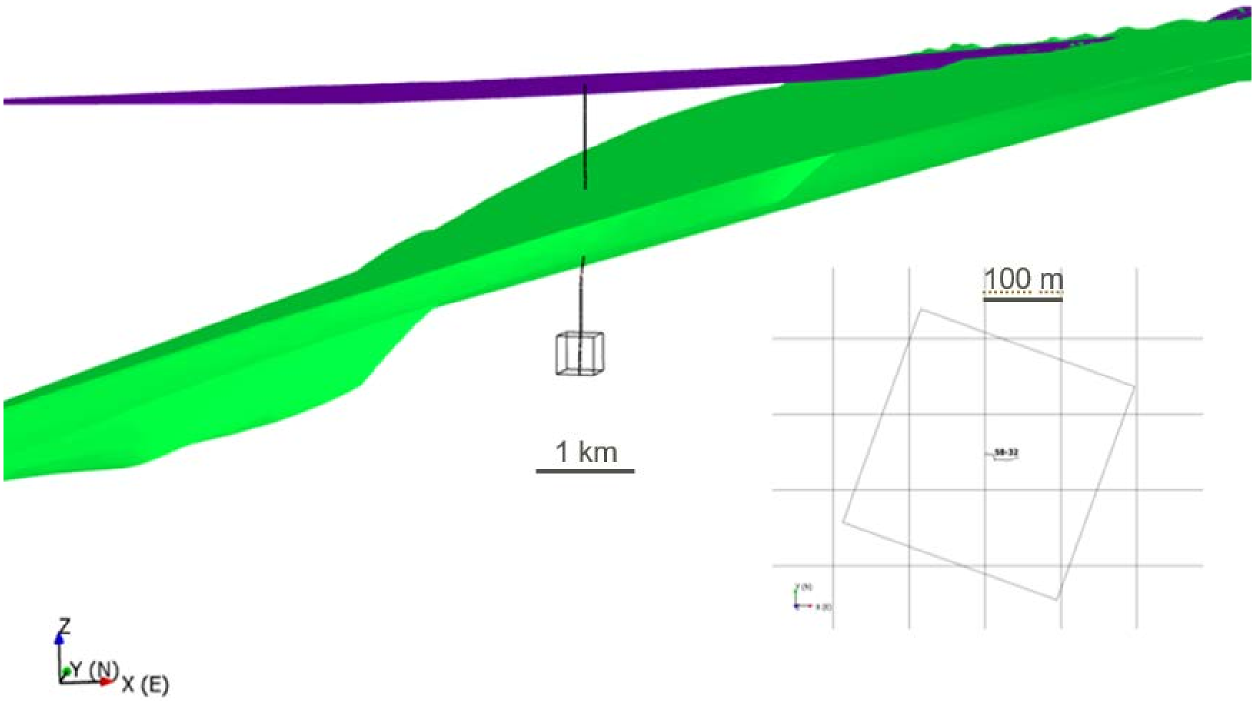

Figure 1: Region for Well 58-32 Zone 2 DFN. The purple surface is ground level while the green surface shows the top of the granitoid bedrock. Enlarged top view in 2D perspective is shown in lower right corner.

Figure 1 shows the region boundaries for the DFN for Well 58-32 Zone 2 where the region box is rotated to align with the principal stress directions with S_{Hmax} being N20E. When the DFN is provided in a local coordinate frame, the region is rotated 20 deg counterclockwise looking down to have the x and y axes aligned with the cardinal directions.

2.2 Stochastic Fracture Set

2.2.1 Fracture Orientation

Four fracture sets have been identified from the FMI data. Three were previously identified from Well 58-32 FMI data. These three were also present in the FMI data from the new vertical well, 56-32, while a new vertical SSW striking set was apparent from the deviated well 16A(78)-32 FMI data. The mean orientations of these sets are listed in Table 1 and shown as black dots on the upper hemisphere stereonets shown in Figure 2.

Table 1: Mean orientations of four fracture sets.

Mean Trend	Mean Plunge	Mean Strike	Mean Dip	Fisher Concentration	Description
88.5	46	178.5	44	15	South striking moderately dipping west
1.5	13.5	91.5	76.5	30	East striking steeply dipping south
131	5	221	85	30	SSW striking vertical
260	17	350	73	10	North striking steeply dipping east

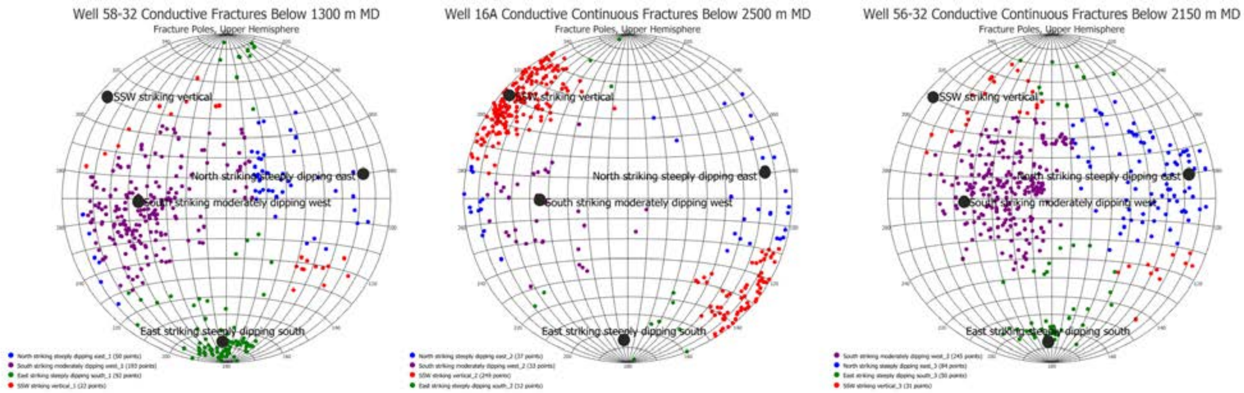

Figure 2: Fracture orientations from FMI data in the deepest portion of the reservoir. Fracture poles are plotted in upper hemisphere stereonets with the color indicating assignment to the nearest mean fracture set pole.

Stochastic fracture sets generated based on these mean set orientations can use the full range of orientations found by using a Fisher distribution with the concentration parameters shown, or they can be "simplified" in order to prevent small angle intersections by only using the mean orientation values. These simplified DFN sets can be more easily meshed when used as input for other modeling software.

2.2.2 Fracture Size and Shape

The fracture size population in the FORGE reservoir can be described by a truncated power law distribution having a power law exponent of 3.2 and a minimum fracture radius of 0.63 m (Finnila, 2021). This fracture size scaling is consistent with both the outcrop data from Salt Cove for fractures having trace lengths in the 40 to 100 m range and the much smaller fractures sampled in the FMI data for Well 58-32.

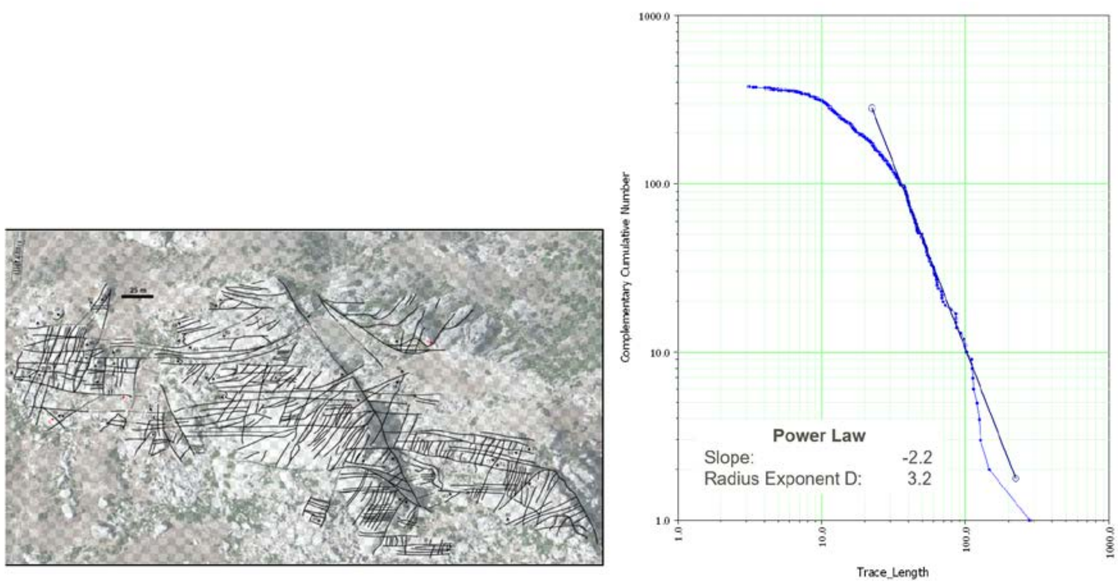

Figure 3: Power law fracture size distribution fit from outcrop trace length data.

Fracture shapes are assumed to be roughly circular and are represented in the DFN as regular hexagons for simplicity as fewer nodes are required in the model to show the extent of each fracture.

2.2.3 Fracture Intensity

Average fracture intensity was estimated in the deep reservoir by integrating the FMI data coming from 58-32, 16A(78)-32, and 56-32. Natural fractures identified in the FMI in the target reservoir depths were sorted into the four sets that were identified based on their orientations. Fracture intensities were first measured as P_{10} values, the number of fractures in the well interval divided by the interval length. This fracture intensity measurement is a function of both the well trajectory and the fracture set orientation, so needs to be converted to a P_{32} fracture intensity, fracture area divided by the volume. This fracture intensity measurement is independent of the well trajectory or fracture orientations and even sizes, so it is a better measure to use when comparing relative fracture intensities. To convert between the P_{10} and P_{32} values, a Terzaghi weight (Terzaghi, 1965) was calculated using a maximum value of 7 and the P_{32} values were then calculated as the sums of the Terzaghi weights in the interval divided by the interval length.

In Table 2, the white cells at bottom row show that the total P_{32} is quite similar between the two vertical wells, 58-32 and 56-32, while the total P_{32} is much lower in 16A(78)-32. This matches the hypothesis that the FMI for 16A(78)-32 is quite biased and only picking up fractures well-oriented to intersect the borehole. To produce average fracture intensities for the four sets, the P_{32} from the two vertical wells was averaged along with just one set from 16A(78)-32 (P_{32} values in italic text were excluded). FMI results from the vertical wells were assumed to sample all the sets reasonably well, while 16A(78)-32 was assumed to only fully sample the SSW striking vertical set. While the vertical wells would also be expected be missing intensity from any vertical sets present, 58-32 at least seems to sample the East striking steeply dipping south set reasonably well so it is unclear why it isn't picking up more of the SSW striking vertical set. Table 3 shows the final mean fracture set intensities used for the DFN in the deep reservoir region.

Table 2. Fracture set intensity by well.

	58-32		**16A(78)-32**		**56-32**	
Description	**P_{32} [1/m]**	**[%]**	**P_{32} [1/m]**	**[%]**	**P_{32} [1/m]**	**[%]**
South striking moderately dipping west	0.34	35.50%	*0.06*	10.30%	0.49	42.50%
East striking steeply dipping south	0.47	49.20%	*0.05*	8.70%	0.23	19.40%
SSW striking vertical	0.05	5.00%	0.38	68.10%	0.14	12.40%
North striking steeply dipping east	0.1	10.30%	*0.07*	13.00%	0.3	25.70%
	0.95		**0.56**		**1.16**	

Table 3: Mean deep reservoir fracture set intensity.

Description	P_{32} [1/m]	[%]
South striking moderately dipping west	0.42	36.1%
East striking steeply dipping south	0.35	30.1%
SSW striking vertical	0.19	16.6%
North striking steeply dipping east	0.20	17.2%
	1.15	**100.0%**

2.3 Deterministic Fracture Set

While a stochastic set of fractures is helpful for estimating unknown fracture populations, it is desirable for some modeling purposes to have the DFN honor the locations and orientations of fractures that have been measured in the FMI log. These are generated in a separate set referred to as the Deterministic Fracture Set. Stochastic fractures intersecting well boreholes where FMI data is available are removed so that synthetic well logs created from the trajectories of the wells will look identical to the measured ones. While this fracture set is deterministic in the sense that the general fracture locations and orientations are known to some extent, the fracture sizes, shapes and exact locations of the centers of the fractures are still randomly generated, so that different realizations of the fracture set are also possible. Figure 4 shows this workflow for the Well 58-32 Zone 2 DFN where simplified orientations were used for the four sets and the DFN only included fractures having a radius greater than 10 m.

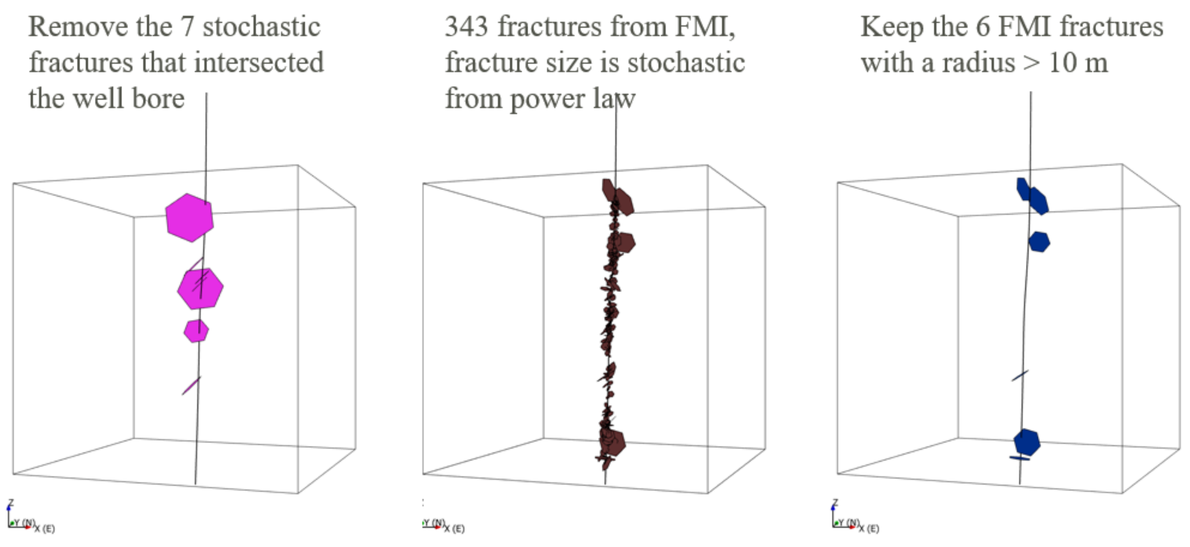

Figure 4: Creation of the deterministic fracture set for DFNs having various minimum fracture size cutoffs.

2.4 Calibration of the Model

There are some whole rock measurements available for porosity, permeability and compressibility. Once the geometrical aspects of the fractures are parameterized for the DFN such as size, shape, orientation and intensity, those properties that contribute to the whole rock properties are assigned so as to make the model consistent with these observations.

2.4.1 Fracture Aperture

Natural fracture apertures are quite complicated and can be defined in different ways. The DFNs for the FORGE site use two different ones: a mechanical aperture which contributes to the fracture porosity, and a hydraulic aperture which controls fracture hydraulic permeability. Information about the mechanical aperture comes from aperture estimates from the FMI data in Well 58-32 shown in Figure 5. Information about the hydraulic aperture comes from the well tests performed on Well 58-32 and the modeling work performed to match these tests (Xing et al., 2021). The hydraulic apertures are found to be 1-2 orders of magnitude smaller than the mechanical apertures measured from FMI (Figure 6).

In the DFN, the mechanical aperture is assigned by assuming a relation between the aperture and the fracture size. Larger fractures will have larger apertures. The bulk porosity is a combination of the fracture porosity and the matrix porosity and so is an upper bound on the fracture porosity. Lab measurements of porosity from core samples was less than 0.5% (McLennan et al., 2018). For this calibration, we assume that the aperture is linearly related to the square root of the fracture radius, R. This relation is often useful in a DFN where fractures are treated as planar features having a constant aperture.

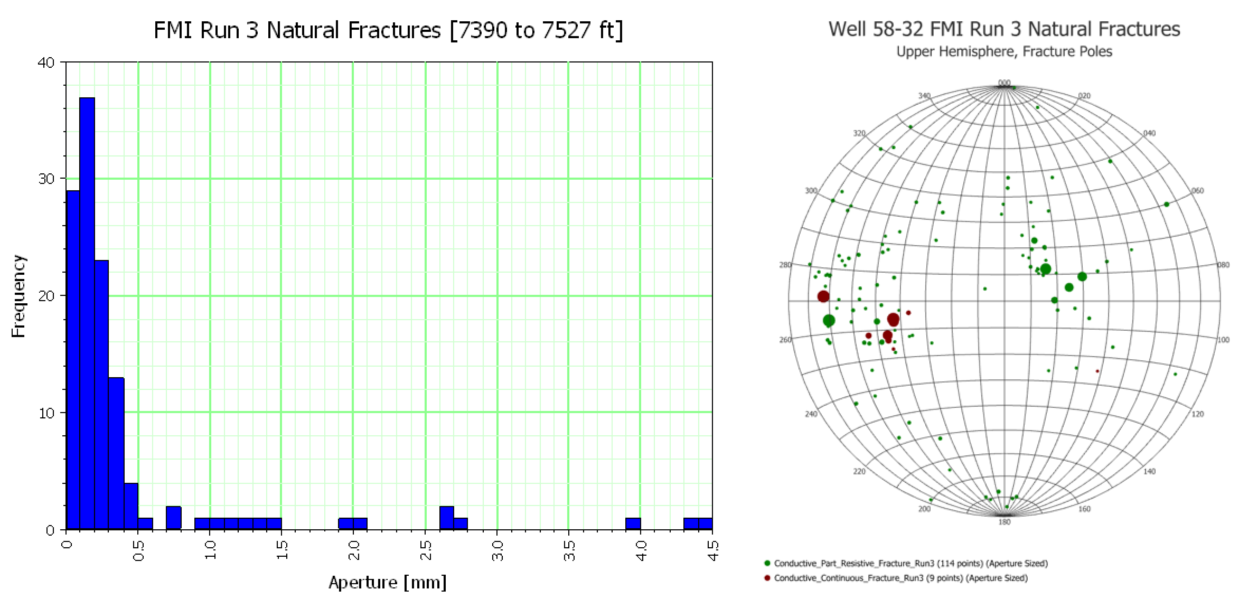

Figure 5: Mechanical apertures and fracture orientations from Well 58-32 FMI data. Upper hemisphere stereonets shows fracture orientations with the size of the dot for the fracture pole showing relative aperture sizes.

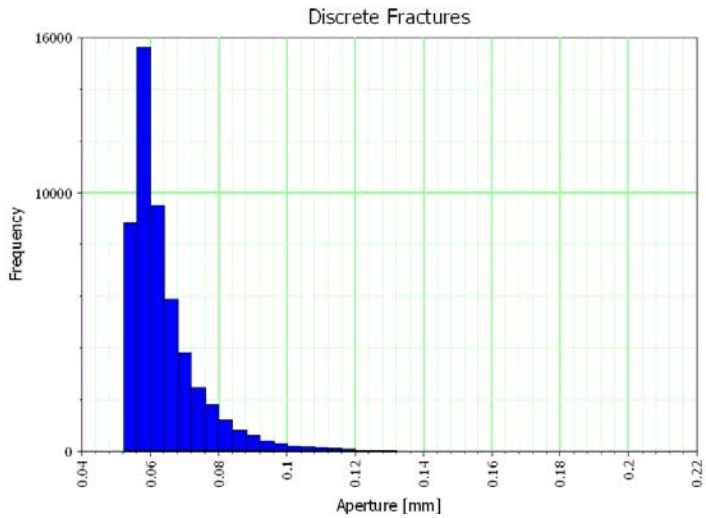

Figure 6: Hydraulic apertures assigned to Well 58-32 Zone 2 DFN.

2.4.2 Fracture Compressibility

The method for calibrating fracture compressibility remained the same as was used in the previous FORGE reference DFN and is based on measurements of Young's Modulus, E, and Poisson's Ratio, ν, in the granitoid. Rock compressibility, β, is defined as the inverse of the bulk compressibility and can be represented with these two other elastic moduli (Birch, 1961):

$$\beta = \frac{3(1-2\nu)}{E} \tag{1}$$

Using E equal to $4.5x10^{10}$ Pa and ν equal to 0.25 (Moore et al., 2018), the rock compressibility is $3.3x10^{-5}$ 1/MPa. When upscaling from a DFN, the rock compressibility is defined as:

$$\beta = \beta_F * \phi_F \tag{2}$$

where β_F is the fracture compressibility and φ_F is the fracture porosity (Golder, 2021). Since the fracture apertures have already been calculated, the fracture porosity can be determined through upscaling the DFN. Combining equations 1 and 2 then yields a mean fracture compressibility of $7.2x10^{-3}$ 1/MPa.

2.4.3 Fracture Permeability

The average rock in-situ permeability of the granitoid is estimated to be $4.7x10^{-17}$ m^2 from well testing performed in Phase 2B (McLennan et al., 2018). In a similar workflow as was utilized to estimate fracture apertures, a relationship between fracture permeability k_F, and aperture, e, is assumed:

$$k_F = be^{1.5} \tag{3}$$

Where b is a constant that needs to be empirically determined. Using a value of b equal to $3.13x10^{-15}$ for the fractures in the reference DFN yields permeabilities in the cell coordinate directions IJK of $4.6x10^{-17}$ m^2, $4.6x10^{-17}$ m^2, and $4.9x10^{-17}$ m^2 respectively.

3. DFN Subsets and Availability

The DFNs described in the paper are available on the GDR in both the global coordinates and local coordinates. The individual discrete fractures are available in different size ranges and upscaled values are provided for the smaller fractures that are not explicitly represented.

3.1 Discrete Fracture Sets

With millions of fractures potentially generated in the reference DFN for the largest modeling region, it can be useful to provide various subsets depending upon the desired purpose. Some common subsets are to filter the fractures by size to only consider the largest ones, or to perform a critical stress analysis on them and only select the ones which show high values of critical stress. In both cases, it is generally assumed that these subsets will include the most hydraulically significant fractures. Some subsets have been filtered to only include fractures that are connected to the well(s) of interest.

3.2 Upscaled DFN Properties

In order to assist continuum modeling, the DFN is also upscaled to provide bulk rock values for such parameters as porosity, directional permeability, and sigma factor. The properties can be averaged over varying length scales as needed. These properties can be transferred to other simulators using grid file formats or point data having associated mean property values. Figure 7 shows how fracture porosity from small, background fractures can be combined with upscaled large discrete fractures to provide a model suitable for continuum modelers.

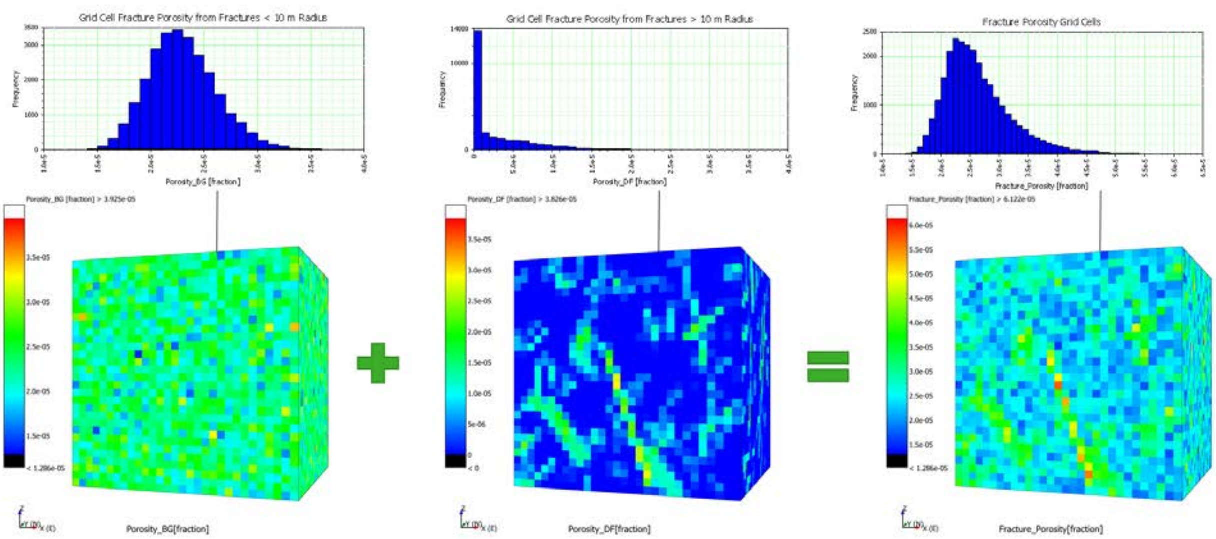

Figure 7: Upscaled porosity values for Well 58-32 Zone 2 DFN.

4. Conclusion

In addition to providing the three DFN realizations consisting of individual fractures, a more general description of the fracture sets is provided in tabular form in the paper. These summary set orientations, intensities, and size parameterizations can be used to generate additional, compatible DFN representations of the FORGE reservoir.

Acknowledgement

Funding for this work was provided by the U.S. DOE under grant DE-EE0007080 "Enhanced Geothermal System Concept Testing and Development at the Milford City, Utah FORGE Site". We thank the many stakeholders who are supporting this project, including Smithfield, Utah School and Institutional Trust Lands Administration, and Beaver County as well as the Utah Governor's Office of Energy Development.

REFERENCES

Birch, F. "Velocity of compressional waves in rocks to 10 kilobars, Part 2." *J. Geophys. Res.*, 66, (1961), 2199-2224.

Energy and Geoscience Institute at the University of Utah. "Roosevelt Hot Springs, Utah FORGE Final Topical Report 2018" [data set]. Retrieved from http://gdr.openei.org/submissions/1038, (2018).

Finnila, A., Forbes, B., and Podgorney, R. "Building and Utilizing a Discrete Fracture Network Model of the FORGE Utah Site." *Proceedings, 44th Workshop on Geothermal Reservoir Engineering*, Stanford University, Stanford, CA (2019).

Finnila, A. "Estimation of Fracture Size for a Discrete Fracture Network Model of the Utah FORGE Geothermal Reservoir using Forward Modeling of Fracture-Borehole Intersections." Paper presented at the 55th U.S. Rock Mechanics/Geomechanics Symposium, physical event cancelled, June 2021. Originally accepted for the 3rd International Discrete Fracture Network Engineering Conference. DFNE 21-2329 (2021).

Golder Associates: FracMan® Reservoir Edition, version 8.1 Discrete Fracture Network Simulator, (2021).

McLennan, J., Nadimi, S., Trang, T. and Forbes, B. "Permeability Measurements, FORGE Utah Technical Report." Report to Department of Energy, Geothermal Technologies Office, April 2018, (2018).

Moore, J., McLennan, J., Handwerger, D., Finnila, A., and Forbes, B. "Mechanical Property Measurements, FORGE Utah Technical Report." Report to Department of Energy, Geothermal Technologies Office, April 2018, (2018).

Terzaghi, R.: Sources of Error in Joint Surveys, *Géotechnique*, **15**, (1965), 287-304.

Xing, P., Damjanac, B., McLennan, J., Radakovic-Guzina, Z., Finnila, A., Podgorney, R., and Moore, J. "Numerical Simulation of Injection Tests at Utah FORGE Site." *Proceedings, 46th Workshop on Geothermal Reservoir Engineering*, Stanford University, Stanford, CA (2021).